


FDTD Simulation Study of Brillouin Scattering Emission Lines Stimulated by High Frequency Radio Waves in the Ionospheric Plasmas

Barzegar, S.¹ 

1. Department of Space Physics, Institute of Geophysics, University of Tehran, Tehran, Iran.

Corresponding Author E-mail: sbarzegar@ut.ac.ir

(Received: 7 July 2024, Revised: 15 Feb 2025, Accepted: 5 March 2025, Published online: 15 March 2025)

Abstract

A high-power electromagnetic (EM) wave can decay into an ion acoustic wave and a scattered EM wave in a plasma through a process called Stimulated Brillouin Scattering (SBS). A one-dimensional fully electromagnetic Finite-Difference Time-Domain (FDTD) method is used in a magnetized plasma with an increasing density ramp to simulate the propagation of a linearly polarized high-frequency (HF) radio wave traveling through the plasma along magnetic field lines. The study shows that the plasma splits the linearly polarized EM wave into two separate counter-rotating circularly polarized waves: the X-mode and the O-mode waves. The specific cutoff points for each of these circularly polarized waves are illustrated, with the X-mode reflecting at lower frequencies compared to the O-mode. As the radio wave approaches the cutoff frequency, it decays into a scattered high-frequency EM wave and a low-frequency wave. By analyzing the frequency spectrum of the scattered wave and the excited electrostatic low-frequency wave, the electrostatic wave is identified as an ion-acoustic (IA) mode, thus confirming the process as SBS. The growth rate of the excited longitudinal electrostatic wave is studied by calculating the excited longitudinal wave energy. The evolution of energy transfer and conversion from the HF wave to IA wave, as well as electron and ion kinetic energy, is investigated. The results indicate that electron and ion density perturbations experience similar fluctuations.

Keywords: Ion-Acoustic Wave, HF wave, Ionosphere, O-mode, X-mode.

1. Introduction

HF radio waves can heat the ionosphere's F-layer through interactions with ionospheric plasma. This process is facilitated by ground-based ionospheric heaters used for artificial heating experiments (Kuo et al., 2010; Lukianova et al., 2019; Chilson et al., 2000). The artificial heating can cause disturbances in temperature, density, and other parameters of the ionospheric plasma. Consequently, various wave modes such as electron waves, lower hybrid waves, ion-cyclotron waves, and ion-acoustic waves, can be excited in the plasma. These modes contribute to SBS or Stimulated Raman Scattering (SRS) of incident HF radio waves through the parametric decay process (Jahangiri and Sadighi-Bonabi, 2016; Fu et al., 2013; Eliasson et al., 2021; Labaune and Pesme, 1997; Cheriyan and Krishnan, 2022).

SBS is a nonlinear optical process that occurs when an intense pump wave (such as an HF radio wave) interacts with a medium like plasma, leading to the generation of a scattered wave and an IA wave (Niknam et

al., 2013; Mahmoudian et al., 2013). Generally, SBS can be used to probe the medium's properties, making it a useful tool for remote sensing in space plasmas. The interaction of HF radio waves with ionospheric plasma can reveal information about its density, temperature, and other characteristics. Since the SBS from an incident HF radio wave can propagate tens of kilometers without significant attenuation, and the process is sensitive to the conditions of the ionosphere, it is an appropriate diagnostic tool for space science research and remote sensing applications.

SBS in the ionosphere involves the interaction of HF radio waves as a pump wave with the ionospheric plasma. When an HF wave propagates through the ionosphere, it can excite electrostatic IA waves. As the pump wave approaches its corresponding cutoff point, the electric field grows to a value exceeding the threshold for parametric decay into a scattered HF EM wave and a low-frequency electrostatic wave, such as IA

Cite this article: Barzegar, S. (2025). FDTD Simulation Study of Brillouin Scattering Emission Lines Stimulated by High Frequency Radio Waves in the Ionospheric Plasmas. *Journal of the Earth and Space Physics*, 50(4), 179-189. DOI: <http://doi.org/10.22059/jesphys.2025.378487.1007614>

wave. The excited acoustic waves, in turn, can scatter the incident HF wave into a Stokes/anti-Stokes wave, which has a lower/higher frequency due to energy transfer to the acoustic wave. The wave frequency and wave vector direction obey the energy and momentum conservation equations: $\omega_0 = \omega_s + \omega_{IA}$, $k_0 = k_s + k_{IA}$, where ω_0/k_0 , ω_s/k_s , and ω_{IA}/k_{IA} are the frequency/wave numbers for the incident HF pump, scattered HF wave, and ion-acoustic wave, respectively (Kruer, 1988; Eliezer, 2002.; Kaw and Singh, 2017). SBS can be used to study the ionosphere by analyzing the frequency shift and intensity of the scattered waves, which carry information about the plasma's density fluctuations and sound speed. This makes SBS a valuable tool for remote sensing and understanding space weather phenomena (Stenflo, 1990). The efficiency of SBS depends on various factors, such as the intensity of the incident wave, the properties of the ionospheric plasma, and the angle of incidence (Bernhardt et al., 2009).

SBS in the ionosphere, particularly in the context of HF radio waves, has been the subject of several studies. Numerous studies have made significant progress in understanding the behavior of SBS in the ionosphere. Dysthe et al. (1977) discuss the possibility of obtaining stimulated backscattering from the ionosphere. It is found that SBS of ion modes and quasi-modes may be possible with the signal power planned for the EISCAT radar. Norin et al. (2009) reported unprecedentedly strong and narrow EM emissions, attributed to SBS, in experiments at the High-Frequency Active Auroral Research Program (HAARP) in Alaska. Bernhardt et al. (2010) further explored the role of magnetized SBS in producing low-frequency electrostatic waves, with implications for ion composition measurements. Bernhardt et al. (2009) used the SBS technique to measure electron temperatures in the modified ionosphere over HAARP, providing valuable insights into the heating effects of HF radio waves. These studies collectively contribute to a deeper understanding of SBS in the ionosphere and its potential applications. Mahmoudian *et al.* (2013) discuss the potential for SBS in the ionosphere, specifically noting the suppression of SBS emission sidebands as the HF pump frequency is stepped across electron

gyro-harmonics. These studies collectively underscore the potential for SBS in the ionosphere and its diagnostic applications. Recent studies continue to refine our understanding of this process, with a focus on optimizing the efficiency and control of SBS processes. The use of advanced simulation tools can further enhance our understanding of SBS.

In this research, we explore the physics behind the MSBS parametric process occurring for an HF radio frequency wave propagating inside magnetized ionospheric plasma using a one-dimensional space and three-dimensional velocity full EM FDTD method. The HF radio wave is chosen to be incident on increasing density magnetized plasma and propagates parallel to the magnetic field. This particular geometry supports the propagation of Right-hand (R) and/or Left-hand (L) circularly polarized EM waves (Kruer, 1988), which correspond to X-mode and O-mode, respectively. In fact, the presence of a strong intrinsic magnetic field makes the ionosphere an anisotropic medium, resulting in the double refraction of an incident EM wave. It is shown that the EM radio wave splits into O-mode and X-mode waves. Then, the parametric decay of the O-mode HF wave into an electrostatic wave (IA) and a scattered HF wave through the SBS process is studied. The resulting SBS emission frequency spectrum is distinguished by its frequency, and IA emission lines appear with a frequency offset from pump wave frequency.

This research is essential because it provides a deeper understanding of how HF radio waves interact with ionospheric plasma, leading to significant implications for space science and communication technologies. The findings show that plasma heating and the excitation of IA modes begin when the pump wave starts backscattering from the cutoff point. The HF wave power provided by available facilities is not sufficient (beyond a certain threshold) to trigger a parametric instability at a density less than $n_{cr}/4$ (Eliezer, 2002). However, at the cutoff frequency point, where the backscattered and incident HF waves interfere, the resulting wave becomes strong enough to excite electrostatic ion modes. The excited IA modes are not strong, and the electron and ion density fluctuations exhibit a sinusoidal form, attributed to the weak excitation of the IA mode.

The manuscript has been organized as follows. Section 2 provides the simulation methods and details. In Section 3, we present the details of observations made by simulating the incident HF radio frequency wave through an ionospheric plasma. The observations have been analyzed in detail in this section, providing evidence of the occurrence of parametric Brillouin backscattering process. We summarize and conclude in Section 5.

2. Methods

We employed the FDTD simulation model, which couples the plasma momentum equation (Equation 1), Faraday's law (Equation 2), and Ampere's law (Equation 3) (Pokhrel and Faruque, 2018; Smith et al., 2020):

$$\frac{\partial J_j}{\partial t} = \epsilon \omega_{pj}^2 E - \omega_{cj} \times J_j, \quad (1)$$

$$\nabla \times E = -\frac{\partial B}{\partial t}, \quad (2)$$

$$\nabla \times H = \frac{\partial D}{\partial t} + \sum J_j. \quad (3)$$

where J_j represents the plasma current density due to each j -species (the subscript j represents electrons, positive ions, etc.), ϵ is the electrical permittivity of the medium, ω_{pj} is the plasma frequency, and ω_{cj} is the cyclotron frequency. The plasma is cold, and no thermal pressure is considered. Therefore, the momentum equation for each species is simplified to Equation (1). The schematic of the model is shown in Figure 1. In this method, we first determine the initial particle momenta, positions, and EM fields. Then, the initial current density (J_j) is calculated. Using Equation (1), (J_j) is updated and incorporated into Equations (2) and (3), which are solved using the FDTD method. This method is efficient for large-scale simulations.

This simulation method is employed to study the HF radio wave propagation through plasma under conditions similar to those of the ionosphere. Table 1 provides the HF radio wave and plasma simulation parameters. The Earth's uniform magnetic field amplitude of $B = 50 \mu\text{T}$ is considered along the z -direction. The presence of a strong intrinsic

magnetic field makes the ionosphere an anisotropic medium, resulting in the double refraction of an incident EM wave. In our study, the initial HF wave is linearly polarized, and its propagation direction is along the magnetic field (z -direction). The propagation along the magnetic field lines can be a good approximation since the dip angle variation is insignificant over the horizontal extent. In addition, the excitation of a pure IA mode, which is the purpose of this study, occurs when the incident EM wave is directed along the magnetic field (Fu et al., 2013).

A 1-D simulation box in the z -direction with dimension $L_z = -53$ to 53 km is chosen. The plasma density profile $n(z)$ is initialized from zero (at $z = 0$ km) and linearly increases to $2n_{cr}$ (at $z = 53$ km), where, $n_{cr} = n_0 = 2.5 \times 10^5 \text{ cm}^{-3}$ is the electron density that satisfies $\omega_{p0} = \omega_0$. The plasma frequency at n_0 (at $z = 26.5$ km) is given by $\omega_{p0} = (n_0 e^2 / m_e \epsilon_0)^{1/2}$. Frequencies are normalized by the electron plasma frequency, lengths by the electron skin depth ($k_{p0} = \omega_{p0} / c$), and the electric and magnetic fields by $m_e c \omega_{p0} / e$, where c , ϵ_0 and e are light velocity, permittivity, and electron charge, respectively. The range of the plasma frequency to electron gyrofrequency ratio is $0 \leq \omega_p / \omega_{ce} \leq 6.24$. The density gradient scale length (L_n) is given by $L_n = \left| \frac{n_e}{\nabla n_e} \right| = 26.5$ km.

The number of superparticles per cell is 20 for electrons and 20 for ions, and an open boundary condition is considered for particles. The spatial resolution is taken as 1 m (equal to 106000 grid points), and Maxwell's equations and the plasma momentum equation are updated using time step increment of $\Delta t = 1.4$ ns. This value is chosen to satisfy the Courant limit (the upper limit of the allowable time-stepping increment for solving Maxwell's equations using FDTD to ensure numerical stability) (Taflove and Hagness, 2005; Pokhrel and Faruqu, 2018). These conditions ensure the model avoids numerical dispersion and instabilities. The model simulates $700 \mu\text{s}$ in real time.

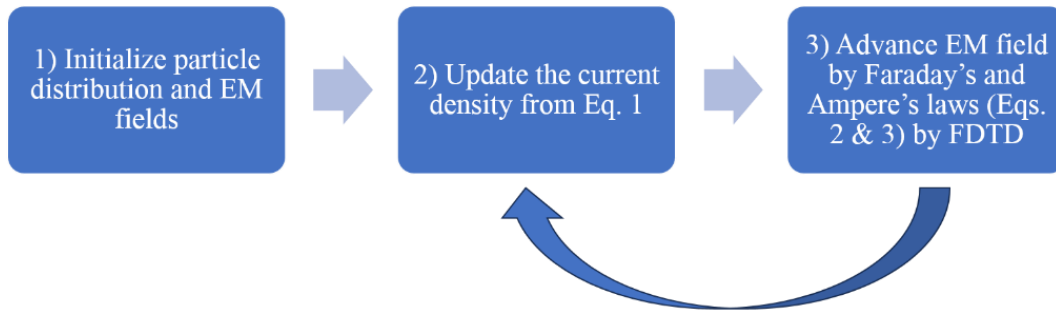


Figure 1. The basic loop of hybrid FDTD-PIC simulations.

The HF radio wave is modeled as a plane wave because the region of the ionosphere is far away from the ground antenna. The HF wave is considered to be incident normal to the plasma surface from the left side of the simulation box. Its intensity ($I = 700 \frac{W}{m^2}$) is chosen higher than the available transmitter's power to reduce computational time; however, it is small enough that relativistic effects are absent. Boundary conditions for EM fields are taken as absorbing in the longitudinal direction.

We have followed the dynamics of both electrons and ions. The dominant ion population in the ionosphere is Oxygen; however, to reduce the computational time, we carried out the simulations for a reduced mass of ions, which is chosen to be 4000 times heavier than electrons, $m_i = 4000m_e$, where m_i and m_e represent the rest mass of the ion and electron species, respectively. The simulations were carried out for the case of a cold plasma. What plays the role of effective temperature for exciting an IA perturbation in the Brillouin process is the initial energy acquired by the electrons as a result of ponderomotive pressure from the incident HF Radio wave.

While a one-dimensional simulation cannot account for effects occurring perpendicular to the direction of propagation, such as transverse instabilities and variations across the magnetic field lines, it remains a practical choice for this study. This approach is used because we are dealing with HF wave propagation along magnetic field lines. The magnetic field strength is substantial ($B_0 = 50 \mu T$), leading to a small electron gyroradius of 8.86 cm, given an electron temperature

typical of the ionosphere ($T = 2000$ K). This small radius justifies simplifying the model to one dimension, as the primary variations occur along the magnetic field direction. Additionally, the IA modes that are excited in the simulation are directed mainly parallel to the background magnetic field and thus have a relatively long wavelength in the transverse direction, ensuring that the essential physics of SBS are captured accurately while reducing computational complexity (Goswami and Kumar, 2022).

3. Results and Discussion

HF waves experience a different amount of refraction in the ionosphere depending on their altitude, which is related to plasma density and propagation direction relative to the background magnetic field. These parameters define how a linearly polarized incident beam converts to R- and L-modes, how these waves propagate through the ionosphere, and at which points cutoff frequency, wave backscattering, and IA wave excitation occur. The HF wave has two distinct cutoff frequencies (defined as where $k \rightarrow 0$), as given by (Goldston and Rutherford, 2020),

$$\omega_{R,L} = \frac{1}{2} \left[\mp \omega_{ce} + (\omega_{ce}^2 + 4\omega_{pe}^2)^{\frac{1}{2}} \right]^{\frac{1}{2}} \quad (4)$$

Here, $+/-$ signs stand for the R/L cutoff frequencies, respectively, and $\omega_{ce} = |eB/m_e|$ represents the electron gyration frequency, where e and m_e are the electron charge and mass, respectively. The cutoffs define the pass- and stop-bands for the propagation of EM waves inside the plasma. In the following sections, we will study each of these cases.

Table 1. Values of simulation parameters in normalized and standard units.

Parameters	Normalized value	Values in SI unit
Plasma Parameters		
n_0	1	$2.5 \times 10^5 \text{ cm}^{-3}$
ω_{p0} (plasma frequency at n_0)	1	$28.3 \times 10^6 \text{ Rad/s}$
ω_{pi} (ion frequency at n_0)	0.01	$28.3 \times 10^4 \text{ Rad/s}$
ω_{ce} (electron gyrofrequency)	0.312	$8.8 \times 10^6 \text{ Rad/s}$
HF Radio Wave Parameters		
ω_0 (HF wave frequency)	1	$28.3 \times 10^6 \text{ Rad/s}$
Intensity	0.02	700 W/m^2

3-1. HF Radio Wave Splitting and Cutoffs

In this section, we will study the conversion of the linearly HF radio wave into X-mode and O-mode. Then, the cutoff frequencies, reflection points, and scattered waves for these modes are shown using the FDTD simulation model. The x-component of the electric field (E_x) is shown at four different times in Figure 2 as a function of z . Subplot (a) shows the linearly polarized incident HF wave (black line) at $\omega_p t = 350$, splitting into two X-mode and O-mode EM waves (red line) at $\omega_p t = 1650$ during propagation in the plasma. In fact, the presence of the magnetic field leads to the double refraction of the incident HF wave. According to Equation (1), there exist two cutoffs: (i) $\omega_0 = \omega_R$ and (ii) $\omega_0 = \omega_L$. The blue line in subplot, (b) shows that the X-wave (at $z = 22 \text{ km}$) and O-wave (at $z = 30 \text{ km}$) are separated because they propagate with different velocities in the plasma. At $\omega_p t = 3750$ the X-mode wave reflects from its cutoff point. The O-mode reaches its cutoff point at $\omega_p t = 6850$ and starts reflecting (green line). Subplot (b) shows the scattering of O- and X-modes. We find the O-mode penetrates to a longer distance through the plasma compared to the X-mode. Note that, to represent the pulse separation and reflection from cutoff points, a short incident HF wave duration is considered instead of a plane wave.

3-2. Characterization of Stimulated Brillouin Scattering

In this section, to obtain more realistic results, we choose to consider only the propagation characteristics of the O-mode through the ionospheric plasma and study the SBS of this mode. The energy evolution of the transverse electric and magnetic fields, the longitudinal electrostatic fields, and the kinetic energy of

electrons and ions are studied. The frequency spectrum of transverse and longitudinal fields is also investigated.

The HF source is a time-dependent plane wave in the form of a Gaussian pulse modulating a sinusoid with a duration of $\tau = 180 \mu\text{s}$. The incident wave is considered a plane wave because the ionospheric plasma is far enough from the transmitter antennas. The energy conversion processes from the O-mode to an electrostatic oscillation and eventually to the electron and ion kinetic energy in the cutoff frequency ($\omega_0 = \omega_L$) have been investigated. In Figure 3(a), we have shown the time evolution of the energy associated with the transverse component of the electric field (red) and magnetic field (green) of the incident HF wave. It is shown that the point where transverse magnetic field reaches its minimum corresponds to the cutoff for the O-mode. As shown by the red line, at this point, the transverse electric field of the incident and backscattered HF waves interfere. At the same time, when the electromagnetic energy decreases, the longitudinal electric field increases (Figure 3(b)). However, it is interesting to note that as time further increases ($t > 8000$), the electromagnetic energy increases again from its minimum value. It is important to note that at this time, the electrostatic energy is in a decreasing trend from its peak value. This indicates that there must be a reverse-conversion process where electrostatic energy gets converted back to electromagnetic field energy. The electrostatic energy does not return to its initial value, and some transverse EM energy is lost. This occurs because, after longitudinal wave excitation, some parts of the electrostatic energy is converted to electron and ion kinetic energy through the wave coupling process, resulting in plasma heating.

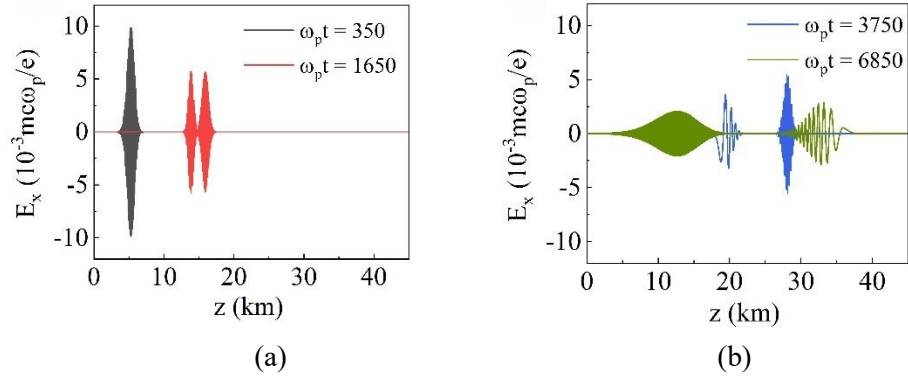


Figure 2. The time evolution of the x-component of the HF wave inside the plasma (at $z > 0$). (a) $\omega_p t = 350$, the HF wave is incident at the plasma. $\omega_p t = 1650$, the pump wave splits into two parts with propagating in the bulk of the plasma. (b) $\omega_p t = 3750, 6850$, further propagation leads to the O- and X-modes scattering from their individual cutoff points, respectively.

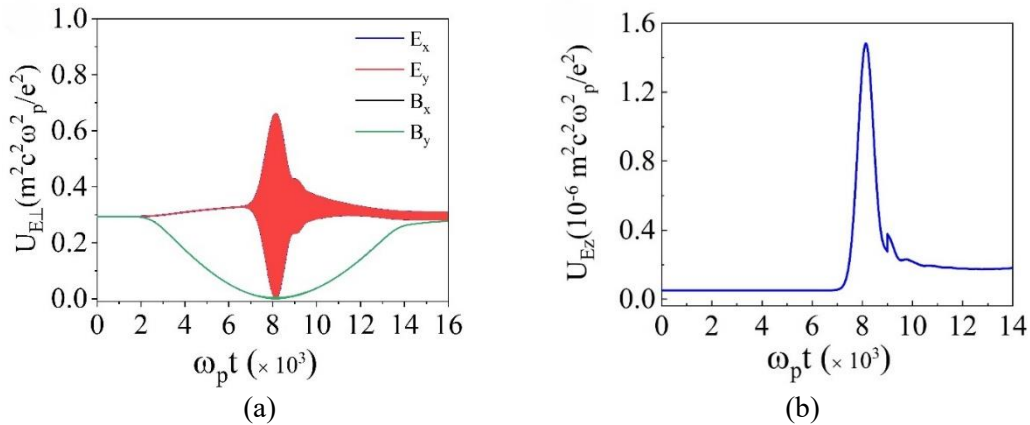


Figure 3. The time variation of spatially averaged transverse electric and magnetic fields and electrostatic energy. Here (a) red and green lines, and (b) blue lines, represent the energy associated with the transverse components of the electric field, magnetic field, and longitudinal electric field, respectively.

The frequency spectra for the electrostatic, electric, and magnetic fluctuations are illustrated in Figure 4. The electric fields are transformed into the frequency domain using the Fast Fourier Transform (FFT). The FFT spectra of the time series data of the longitudinal and transverse electric field components, E_x and E_z , are shown in Figure 4(a) and Figure 4(b). Subplot (a) shows the frequency spectrum of the backscattered wave, which has two peaks. The stronger peak corresponds to the incident HF wave. However, there is another line in subplot (a) with a frequency offset of $0.007\omega_p$ that is related to the electrostatic mode excited in the plasma. By examining subplot (b), it is shown that two electrostatic waves are excited at the reflection point limit over the entire heating cycle. The stronger and lower frequency line appears at $\omega_0 = 0.007\omega_p$, which matches to the IA mode frequency. This IA line has the same frequency as the secondary emission line in subplot (a). Therefore, the SBS is identified in three-wave coupling process. The

SBS line is downshifted from the pump wave (Stokes) and satisfies the Brillouin condition. A very weak line also appears in subplot (b) at frequency $\omega_0 = \omega_p$, which corresponds to the excitation of the electron plasma mode. On the other side, Figures 5(a) and 5(b) represent the spatial FFT of E_z and E_x space series data, respectively. At the reflection point, where $\omega_0 = \omega_L$, based on the EM dispersion relation in a plasma ($\omega_0^2 = \omega_{p0}^2 + k_0^2 c^2$), the pump wave wavenumber is $k_0 = 0$. Figure 5(b) verifies this at the reflection point. This is almost true for the scattered wave, which has a small frequency deviation. Therefore, by the momentum conservation law ($k_0 = k_s + k_L$) for parametric instabilities, the generated longitudinal wave has wavenumber of $k_L \approx 0$ (Figure 5a). The observed bandwidth for k in Figure 5(b) is due to the pump and scattered waves having a certain bandwidth, preventing the wavenumber from becoming zero at a fixed point.

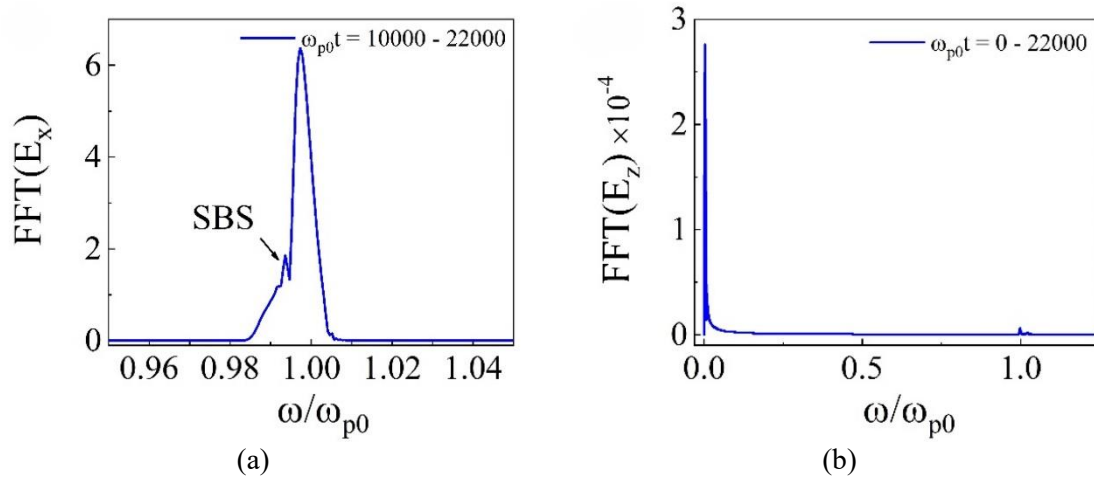


Figure 4. The FFT of (a) scattered wave at $\omega_{p0}t = 10000 - 22000$, $x = -20 \text{ km}$, (b) excited longitudinal wave at $\omega_{p0}t = 0 - 22000$, $x = 39 \text{ km}$, for O-mode HF wave.

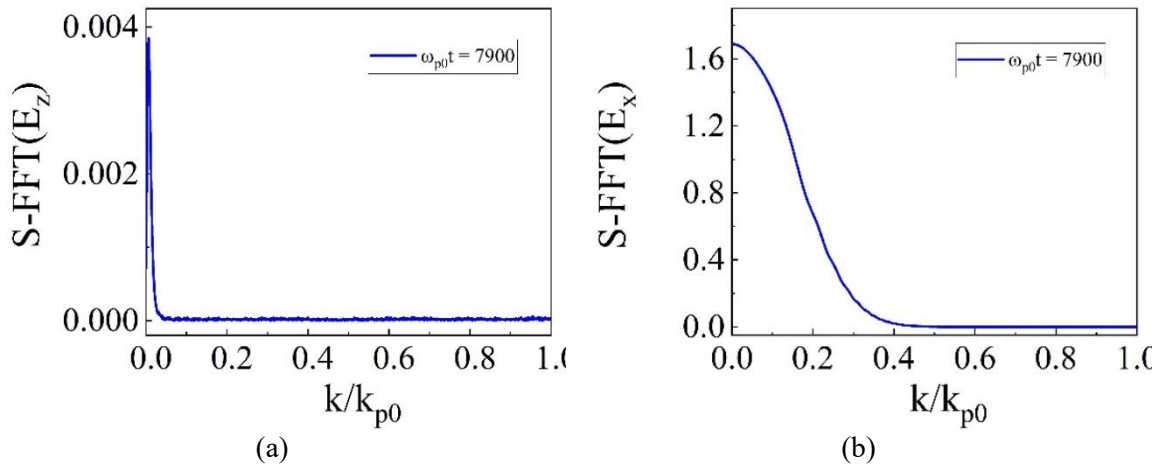


Figure 5. The spatial FFT versus normalized wavenumber of (a) the longitudinal electric field, and (b) the transverse electric field. The FFT is performed at $\omega_{p0}t = 7900$ in the bulk of plasma, during the generation of scattered waves and electrostatic modes.

Since the energy and momentum conservation laws are verified for the pump, scattered, and electrostatic fields, and the electrostatic field frequency is equal to the plasma acoustic frequency, the excited electrostatic field corresponds to the IA mode frequency. Therefore, the SBS is identified through a three-wave coupling process. Figures 6(a) and 6(b) illustrate the wavenumber time evolution of the excited IA mode and the pump and scattered HF radio waves, respectively. Figure

6(b) shows the pump wavenumber decreasing during propagation, becoming zero at the reflection point ($\omega_{p0}t \approx 8000$). The scattered wave then propagates through the plasma, and k_s/k_{p0} increases to approximately 1. At the reflection point, the electrostatic wave is excited with $k_l \approx 0$, and its magnitude decreases over time, leading to damping after a short period (Figure 6(a)). The colorbar in this figure shows the spatial FFT magnitude of the wavenumbers.

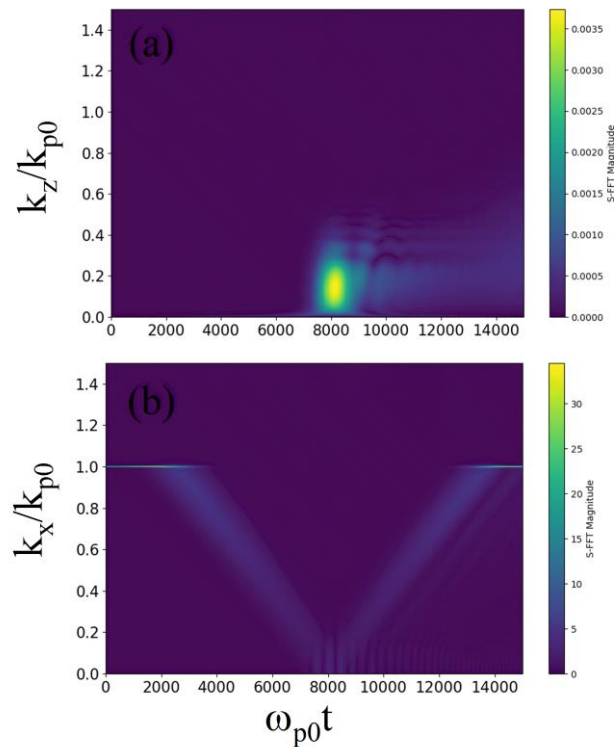


Figure 6. Wavenumber time evolution of (a) the longitudinal electric field, and (b) the transverse electric field during propagation.

To illustrate electron and ion heating more distinctly, we have shown the evolution of averaged electron and ion momentum during the simulation run in Figure 7. Figures 7(a) and 7(b) represent the electron momentum evolution in the z - and x -directions, respectively, while Figures 7(c) and 7(d) show the ion momentum evolution in the z - and x -directions, respectively. Figures 3 and 7 clearly illustrate a complete picture of the energy-conversion process throughout the simulation run. As soon as the HF wave enters the plasma surface, the electron and ion kinetic energy increases. As Figure 3 shows, electrostatic field energy, which was not present before, is also produced at the cost of the electromagnetic energy of the incident wave at the same time. Then, while the incident HF wave propagates through the plasma, the electron and ion kinetic energy, electrostatic energy, and electromagnetic energy remain constant. When the O-mode reaches the cutoff frequency point, the electrostatic energy and electron and ion kinetic energy start to increase, whereas electromagnetic energy decreases.

At the time $\omega_{p0}t \approx 8000$, when the O-mode HF wave has already started reflecting, the electrostatic energy reaches a maximum

value, whereas the electron and ion kinetic energy keeps increasing. Finally, the electron kinetic energy reaches a maximum value, and at the same time, the electromagnetic energy becomes minimal. It is important to note that at this time, the electrostatic energy is in decreasing trend from its peak value, as some of its energy is being converted to electron kinetic energy. However, it is interesting to observe that as time further increases, the electromagnetic energy increases again from its minimum value. At the same time, both electrostatic and electron kinetic energy continue to decrease until they reach saturation. This indicates that there must be a reverse-conversion process where electrostatic energy gets converted to electromagnetic field energy. It is also noteworthy that ions gain kinetic energy of the same order as electrons in the z -direction, which is mostly due to the IA electrostatic wave causing electrons and ions to experience the same fluctuations. However, this is not true in the x -direction.

The corresponding electron and ion charge density fluctuations are shown in Figure 8 for $t = 3800$. It shows that the electron (solid blue line) and ion density perturbations (red dashed line) have similar forms.

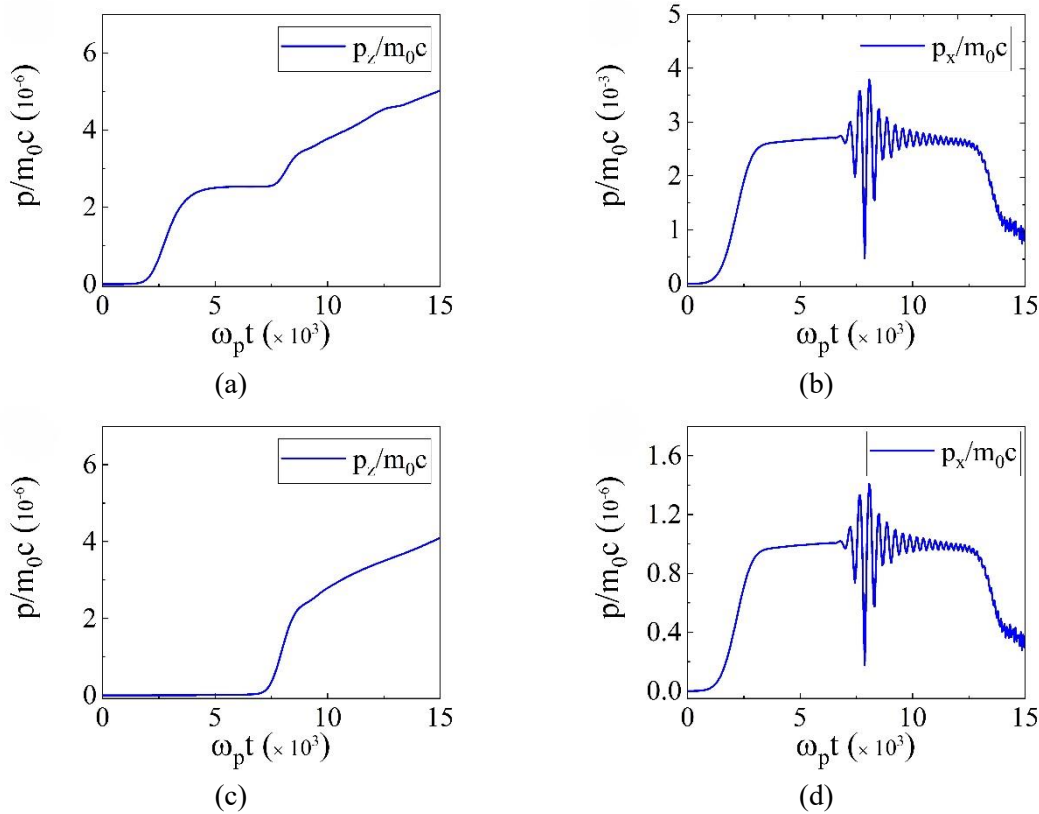


Figure 7. Evolution of (a) averaged electron momentum in the z-direction, (b) averaged electron momentum in the x-direction, (c) averaged ion momentum in the z-direction, and (d) averaged ion momentum in the x-direction.

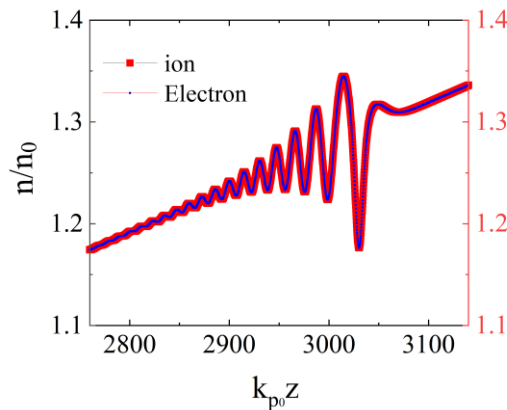


Figure 8. The ion and electron density fluctuations.

4. Conclusion

The present research is an FDTD simulation study of the SBS emission line generation in ionospheric plasmas. The magnetized plasma density profile linearly increases from 0 to $2n_{cr}$. It is shown that the incident linearly polarized HF wave, which is directed along the magnetic field line, splits into two X-mode and O-mode EM waves during propagation in the plasma. The characteristics of the O-mode propagation in the ionospheric plasma are studied. The O-mode wave reflects at the corresponding cutoff frequency. It has been shown that at this point, the HF wave energy

becomes larger than a threshold and is converted to electrostatic energy. This electrostatic mode then converts its energy to electron and ion kinetic energy. The FFT spectra of the backscattered EM wave and the excited electrostatic mode provide evidence the Brillouin scattering process taking place. The frequency spectra show that the frequency of the electrostatic mode is equal to the frequency offset of the stokes backscattered wave. The electron and ion fluctuations are studied, and it is shown that these perturbations have the same form. Our study also reveals that a part of the incident

HF wave excites the IA mode, and a significant portion of its energy is converted to the HF backscattered EM radiation, which is scattered away from the O-mode wave cutoff point.

References

- Bernhardt, P. A., Selcher, C. A., Lehmberg, R. H., Rodriguez, S., Thomason, J., McCarrick, M., & Frazer, G. J. (2009). Determination of the electron temperature in the modified ionosphere over HAARP using the HF pumped stimulated Brillouin scatter (SBS) emission lines. *Annales Geophysicae*, 27(12), 4409–4427.
- Bernhardt, P. A., Selcher, C. A., Lehmberg, R. H., Rodriguez, S., Thomason, J., Groves, K. M., & Frazer, G. J. (2010). Stimulated Brillouin scatter in a magnetized ionospheric plasma. *Physical Review Letters*, 104(16), 165004. <https://doi.org/10.1103/PhysRevLett.104.165004>
- Cheriyann, M., & Krishnan, J. (2022). A comprehensive review on amplification of laser pulses via stimulated Raman scattering and stimulated Brillouin scattering in plasmas. *Plasma*, 5(4), 499–539. <https://doi.org/10.3390/plasma5040037>
- Chilson, P. B., Belova, E., Rietveld, M. T., Kirkwood, S., & Hoppe, U.-P. (2000). First artificially induced modulation of PMSE using the EISCAT heating facility. *Geophysical Research Letters*, 27(23), 3801–3804.
- Dysthe, K. B., Leer, E., Trulsen, J., & Stenflo, L. (1977). Stimulated Brillouin scattering in the ionosphere. *Journal of Geophysical Research*, 82(4), 717–718.
- Eliasson, B., Senior, A., Rietveld, M., Phelps, A. D. R., Cairns, R. A., Ronald, K., Speirs, D. C., Trines, R. M. G. M., McCrea, I., Bamford, R., Mendonça, J. T., & Bingham, R. (2021). Controlled beat-wave Brillouin scattering in the ionosphere. *Nature Communications*, 12, Article 6209.
- Eliezer, S. (2002). *The interaction of high-power lasers with plasmas*. Institute of Physics Publishing.
- Fu, H. S., Kuo, S. P., Kossey, P., & Snyder, A. (2013). Stimulated Brillouin scatter and stimulated ion Bernstein scatter during electron gyroharmonic heating experiments. *Radio Science*, 48(5), 607–616.
- Goldston, R. J., & Rutherford, P. H. (1995). *Introduction to plasma physics*. CRC Press.
- Goswami, L. P., & Kumar, N. (2022). Observations of Brillouin scattering process in particle-in-cell simulations for laser pulse interacting with magnetized overdense plasma. *Physica Scripta*, 97(1), Article 015602.
- Jahangiri, F., & Sadighi-Bonabi, R. (2011). Intense terahertz emission from atomic cluster plasma produced by intense femtosecond laser pulses. *Applied Physics Letters*, 99(26), Article 261501.
- Kaw, P. K., & Singh, S. V. (2017). Nonlinear laser-plasma interactions. *Reviews of Modern Plasma Physics*, 1(1), Article 1. <https://doi.org/10.1007/s41614-017-0005-2>
- Kruer, W. L. (1988). *The physics of laser plasma interactions*. Addison-Wesley.
- Kuo, S. P., Snyder, A., Kossey, P., & Rodriguez, P. (2010). Observation of artificial spread-F and large region ionization enhancement in an HF heating experiment at HAARP. *Geophysical Research Letters*, 37(7), Article L07101.
- Labaune, C., & Pesme, D. (1997). Interplay between ion acoustic waves and electron plasma waves associated with stimulated Brillouin and Raman scattering. *Physics of Plasmas*, 4(2), 423–427.
- Lukianova, R., Kozlovsky, A., & Turunen, T. (2019). First SWARM observations of the artificial ionospheric plasma disturbances and field-aligned currents induced by the SURA power HF heating. *Geophysical Research Letters*, 46(22), 12731–12738.
- Mahmoudian, A., Scales, W. A., Bernhardt, P. A., Fu, H., Briczinski, S. J., & McCarrick, M. J. (2013). Investigation of ionospheric stimulated Brillouin scatter generated at pump frequencies near electron gyroharmonics. *Radio Science*, 48(6), 685–697.
- Niknam, A. R., Barzegar, S., & Hashemzadeh, M. (2013). Self-focusing and stimulated Brillouin back-scattering of a long intense laser pulse in a finite temperature relativistic plasma. *Physics of Plasmas*, 20(12), 122117.
- Norin, L., Leyser, T. B., Nordblad, E., McCarrick, M., & Thidé, B. (2009). Unprecedentedly strong and narrow

- electromagnetic emissions stimulated by high-frequency radio waves in the ionosphere. *Physical Review Letters*, 102(6), 065003. <https://doi.org/10.1103/PhysRevLett.102.065003>
- Pokhrel, S. S., & Faruque, I. (2018). 3-D FDTD modeling of electromagnetic wave propagation in magnetized plasma requiring cold plasma tensor. *IEEE Transactions on Antennas and Propagation*, 66(9), 4772–4781.
- Smith, D. R., Tan, T., Dao, E., Huang, C., & Simpson, J. J. (2020). An FDTD investigation of orthogonality and the backscattering of HF waves in the presence of ionospheric irregularities. *Journal of Geophysical Research: Space Physics*, 125(10).
- Stenflo, L. (1990). Stimulated scattering of large amplitude waves in the ionosphere. *Physica Scripta*, 42(2), 166.
- Taflove, A., & Hagness, S. C. (2005). *Computational electrodynamics: The finite-difference time-domain method* (3rd ed.). Artech House.